CHAPTER 33

THE ENERGY SPECTRA OF SURF WAVES ON A CORAL REEF

by

Theodore T. Lee[1/] and Kerry P. Black[2/]

ABSTRACT

The transformation of waves crossing a coral reef in Hawaii including the probability density function of the wave heights and periods and the shape of the spectrum is discussed. The energy attenuation and the change of height and period statistics is examined using spectral analysis and the zero up-crossing procedure. Measurements of waves at seven points along a 1650 ft transect in depths from 1 to 3.5 ft on the reef and 35 ft offshore were made.

The heights were tested for Rayleigh, truncated Rayleigh and Weibull distributions. A symmetrical distribution presented by Longuet-Higgins (1975) and the Weibull distribution were compared to the wave period density function. In both cases the Weibull probability density function fitted with a high degree of correlation. Simple procedures to obtain Weibull coefficients are given.

Fourier spectra were generated and contours of cumulative energy against each position on the reef show the shifting of energy from the peak as the waves move into shallow water. A design spectrum, with the shape of the Weibull distribution, is presented with procedures given to obtain the coefficients which govern the distribution peakedness. Normalized non-dimensional frequency and period spectra were recommended for engineering applications for both reef and offshore locations.

A zero up-crossing spectrum (ZUS) constructed from the zero up-crossing heights and periods is defined and compared with the Fourier spectrum. Also discussed are the benefits and disadvantages of the ZUS, particularly for non-linear wave environments in shallow water. Both the ZUS and Fourier spectra are used to test the adequacy of formulae which estimate individual wave parameters.

Cross spectra analysis was made to obtain gain function and squared coherency for time series between two adjacent positions. It was found that the squared coherency is close to unity near the peak frequency. This means that the output time series can be predicted from the input by applying the gain function. However, the squared coherency was extremely small for other frequencies above 0.25 H_z.

INTRODUCTION

Most coastal areas of Hawaii, Australia and other tropical regions are protected naturally by a coral reef. Due to complex bathymetry, large energy losses by breaking, friction, scattering and the highly non-linear behavior of impinging waves, the fringing reef presents an extremely complex environment. As a result, the wave transformation on the coral reef is distinctly different from that on sandy coasts. The wave heights, wave

[1/] Researcher, J.K.K. Look Laboratory of Oceanographic Engineering, Department of Ocean Engineering, University of Hawaii, Honolulu, Hawaii

[2/] Formerly Research Associate, Department of Ocean Engineering, and Graduate Student, Dept. of Oceanography, Univ. of Hawaii, Honolulu, Hawaii

periods, and energy spectra are thus modified significantly but information on such a modification is very limited (Bushing, 1976), particularly for correlated field measurements. Knowledge of wave characteristics leeward of a reef is necessary in numerous engineering endeavors, such as the assessment of beach stability, design of coastal structures, prediction of dynamic response of small boats in marinas in waters partly protected by a reef, artificial shoal, and submerged breakwaters. Lack of such knowledge has led to grave uncertainties for designing an economical and sound structure. Also, wave transformation is associated with the living coral environment studied by the marine biologists and wave-induced currents are central to the mechanism of food transformation. This paper will provide some new light concerning the transformation and modification of ocean waves as they progress from deep water through breaking on a reef and on into the shallow water beyond.

FIELD EXPERIMENT

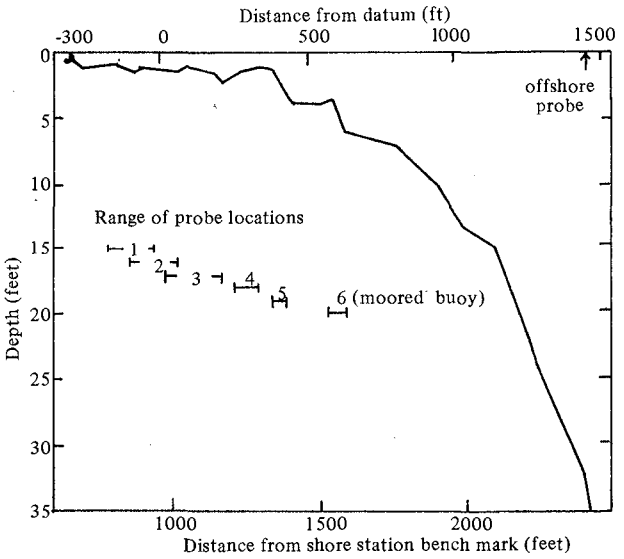

Fig. 1(a) Instrumentation location and bathymetry of Ala Moana reef

Field measurements of water level versus time were made in the ocean at seven points (Fig. 1(a)) along a 1650 ft long transect at the Ala Moana Beach on the southern shore of the island of Oahu (21°17'N, 157°52' W) in Hawaii from July through September 1976. Five capacitance-type probes (numbered 1 to 5, with number 1 most shoreward) were supported on tripods in shallow water on the reef in depths from 1.0 to 3.5 ft. Another capacitance probe (number 9) was mounted on a tower in 35 ft of water (Fig. 1(b)). A floating buoy (number 6) was moored on the outer edge of the reef (6-8 ft depth) and data was recorded by filming the motion of the buoy. The bathymetry with range of location of instruments is shown on Fig. 1(a). All instruments and recording equipment were transported and deployed from a mobile platform equipped with four jack-up legs. At the project site the legs were lowered to the reef to form a fixed platform which allowed the waves to pass underneath. Wave information was cabled back and recorded on a Sangamo Model 3400, 16-channel tape recorder. A portable electric

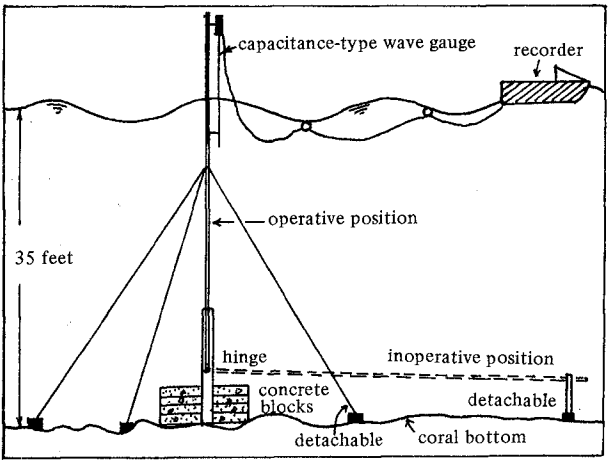

Fig. 1(b) Schematic of offshore wave measurement system

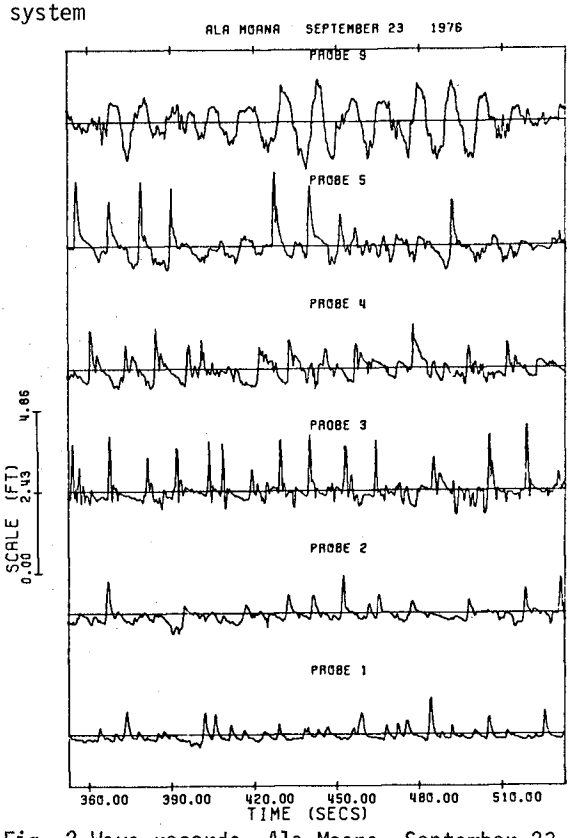

Fig. 2 Wave records, Ala Moana, September 23, 1976.

generator was used as a power source. Offshore data was cabled to a Sanborn strip chart recorder using a catamaran as a recording station.

TIME SERIES

A typical time series is shown on Fig. 2. A qualitative schematic of the wave transformation is shown on Fig. 3. The waves impinging on the reef had primary period of 12 to 18 seconds and significant height up to 3 ft. Offshore, the waves tend to arrive in groups, modulated at a beat frequency. As they shoal on the reef, secondary waves are formed indicative of a highly non-linear process. The shoaling waves typically plunge and produce a saw-tooth profile (Probe 4, Fig. 2). The reformed waves inside the breaker zone have a shortened period, due to the formation of multiple crests.

The random nature of ocean waves is usually described as a stationary Gaussian process. Figures 4 and 5 show the probability density of sea-level elevation against the theoretical Gaussian distribution for offshore and nearshore probes respectively. Note that the shallow water data deviates significantly from the theoretical distribution due to the modified wave profile which has long shallow troughs and peaked crests.

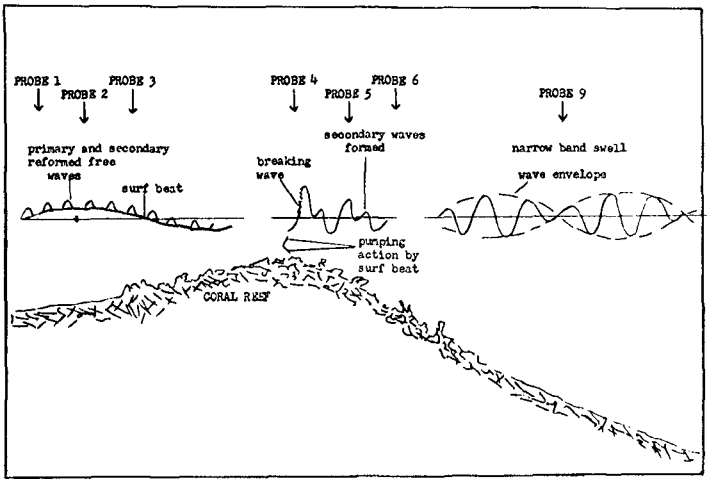

Fig. 3 Qualitative schematic of wave transformation across a reef, with typical probe locations, Ala Moana, 1976.

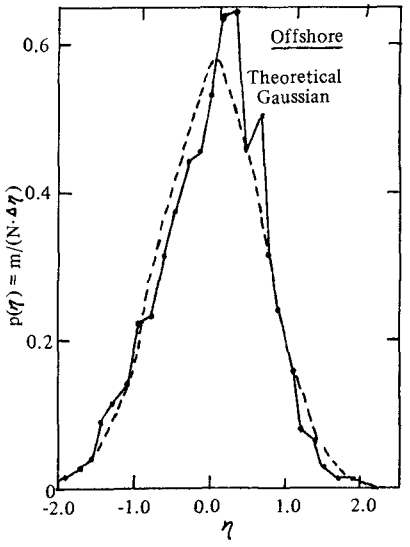

Fig. 4 Probability density of sea level elevation, September 14, offshore probe with Gaussian distribution, Ala Moana, 1976.

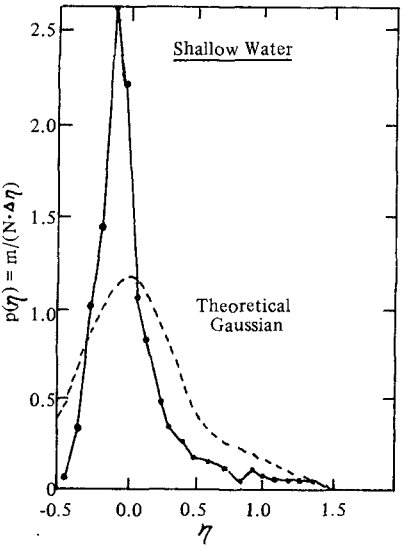

Fig. 5 Probability density of sea level elevation, September 7, probe 4 with Gaussian distribution, Ala Moana, 1976

WAVE HEIGHT

The significant wave height normalized by the offshore significant wave height plotted against the position on the reef is shown on Fig. 6. Due mainly to bottom friction and also to breaking, the ratio decreases

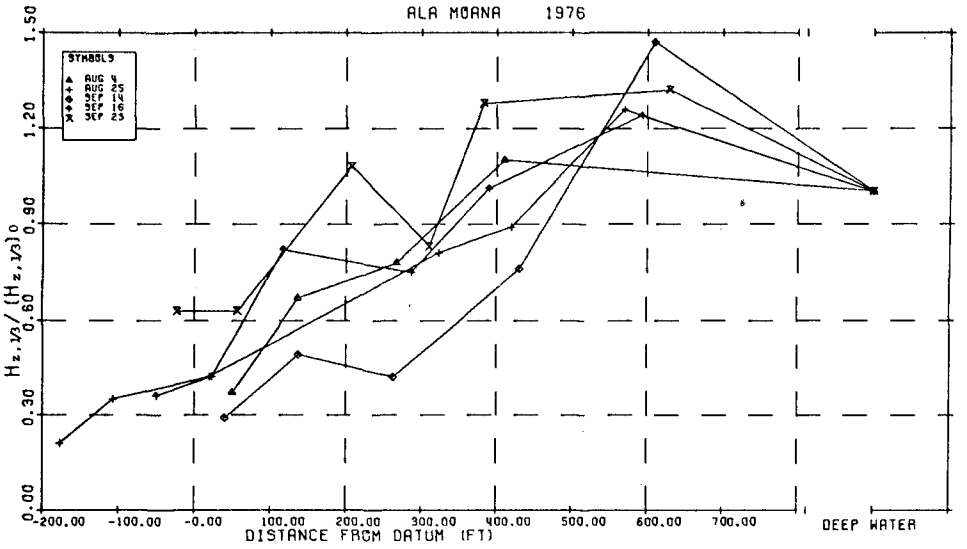

Fig. 6 The significant height normalized by the offshore value against position on the reef, Ala Moana, 1976.

such that the wave height is reduced by approximately 50% every 500 ft travelled on the reef. (The waves generally break at 380 ft from the datum.)

A zero up-crossing analysis was performed on a total on 35 time series and wave height statistics were determined as follows:

$H_{z,1/3}/\overline{H}_z$ =	1.70 ± 0.13	shallow reef	(1)
	1.72 ± 0.11	offshore	
	1.64 ± 0.04	probes exhibiting Rayleigh distribution	
(NOTE:	1.60	theoretical Rayleigh)	
$H_{z,max}/H_{z,1/3}$ =	1.80 ± 0.13	offshore	
	2.60	shoreward of the breaker zone	
	1.60	breaker zone	
(NOTE:	1.74	theoretical ratio given by Longuet-Higgins)	
$H_{z,1/3}/\sigma$ =	3.88 ± 0.52	shallow water	
	3.56 ± 0.13	offshore	
(NOTE:	4.00	theoretical Rayleigh)	

Rayleigh Distribution. In each case, there is significant deviation from the theoretical Rayleigh value. This coincides with a poor fit of the data to the Rayleigh distribution. Typical distributions are shown in Fig. 7. Using a Chi-squared goodness of fit test, the 35 height distributions were compared to the Rayleigh probability density function and 23 did not fit at the 0.025 level of significance. Two out of the five offshore time series did not exhibit Rayleigh distribution due to an excessive number of short period waves (<2 seconds). After filtering of these waves all offshore height distributions were Rayleigh distributed.

Truncated Rayleigh Distribution. The heights were compared to the truncated Rayleigh distribution (Kuo and Kuo, 1975, Battjes, 1974). The

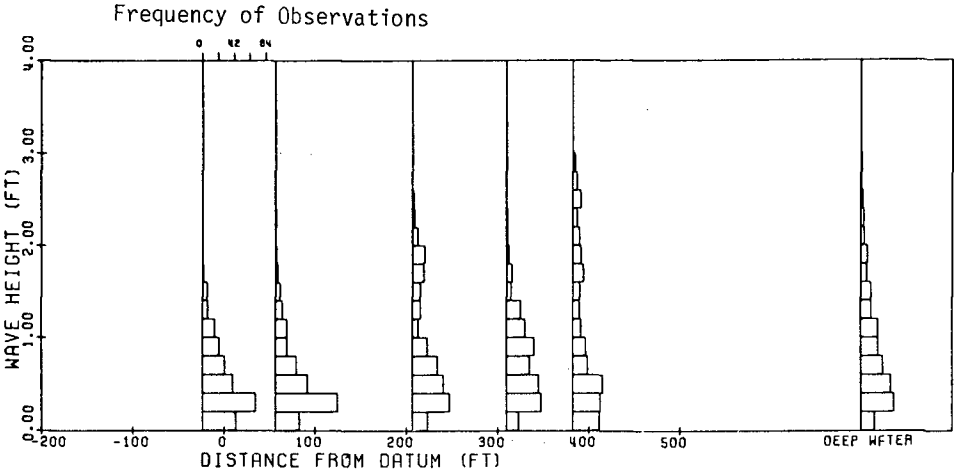

Fig. 7 Distribution of wave heights plotted as height versus frequency of occurrence against position on the reef, Ala Moana, September 23, 1976.

fit was excellent in the breaker zone, but poor both offshore and shorewards of this region. This means that the truncated distribution can only be applicable on certain parts of the reef.

Weibull Distribution. A more general distribution which fits at all positions on the reef for various meteorological conditions was needed. The Weibull distribution given by

$$f(H) = \alpha\beta H^{\beta-1}\exp(-\alpha H^{\beta}) \tag{2}$$

was selected, and the correlation coefficient, ρ_{12}, which is unity for a perfect fit exceeded 0.98 at most positions on the reef. Arhan and Ezraty (1975) also used Weibull distribution successfully to fit their wave data in shallow water.

It should be noted that Rayleigh is a special case of the Weibull distribution with $\beta=2$ and $\alpha=1/H^2_{rms}$. Procedures to determine β (peakedness coefficient), and α follow:

(1) Curve fitting.

The probability of exceeding $x=x_n$ is

$$G(x_n) = \int_{x_n}^{\infty} f(x)dx = \exp(-\alpha x_n^{\beta}) = n/N \tag{3}$$

where n waves exceed x_n of a total of N waves. Taking logarithms twice gives

$$\ln[\ln(N/n)] = \ln(\alpha)+\beta\ln(x_n) \tag{4}$$

which is a linear equation with intercept at $\ln(\alpha)$ and gradient β. The coefficients β and α can be determined using standard linear regression techniques or by plotting the double logarithm term against $\ln(x)$ and fitting a straight line.

(2) Distribution width function.

The distribution width function is defined (Black, 1978) as

$$Q_H = 4 \int_0^\infty H\, f(H)^2 dH \tag{5}$$

For a Weibull distribution.

$$Q_H = \beta \tag{6}$$

The approximate value of β for data divided into bins of width ΔH

$$Q_H = \beta = \frac{4}{N^2 \Delta H} \sum_{i=1}^{NBINS} H_i m_i^2 \tag{7}$$

where N is the total number of waves, NBINS is the number of bins, and H_i and m_i are the heights and number of occurrences respectively in the i^{th} bin. The squared probability density term in the distribution width function tends to magnify small deviations from the theoretical distribution and Q_H is sensitive to the choice of the number of bins which should be selected such that

$$NBINS < N/10$$

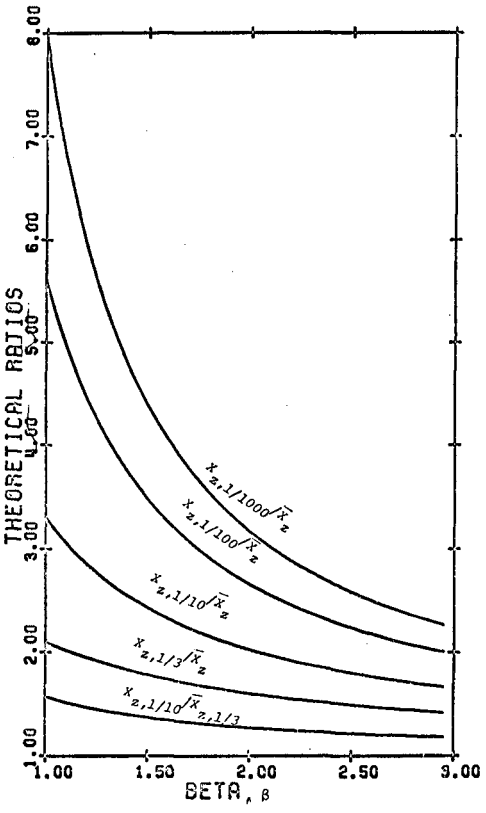

Fig. 8 Theoretical ratios of wave height (period) statistics for waves exhibiting the Weibull distribution against beta, β. (X may be height or period.)

(3) Determination of β without curve fitting.

The ratio of two height (or period) statistics is uniquely defined by the peakedness so β may be easily determined using any two statistics such as $H_{z,1/3}/\bar{H}_z$ or $\sigma(H)/\bar{H}_z$ (which are most stable). To facilitate this approach, the theoretical values of several ratios were plotted against β (Fig. 8). One enters the figure with any of the ratios and reads β. The theory is derived by Black (1978).

Procedures to determine the other coefficient, α, follow:

(i) The Weibull coefficient α may be determined as

$$\alpha = [\Gamma(1 + 1/\beta)/\bar{H}_z]^\beta \tag{8}$$

where Γ is the gamma function, and $\bar{H}_z$ is the mean height of the distribution. Figure 9 presents a family of curves for various α using Eq. (8). α may be determined if one enters the figure with β and $\bar{H}_z$.

(ii) Another useful equation to determine α which does not

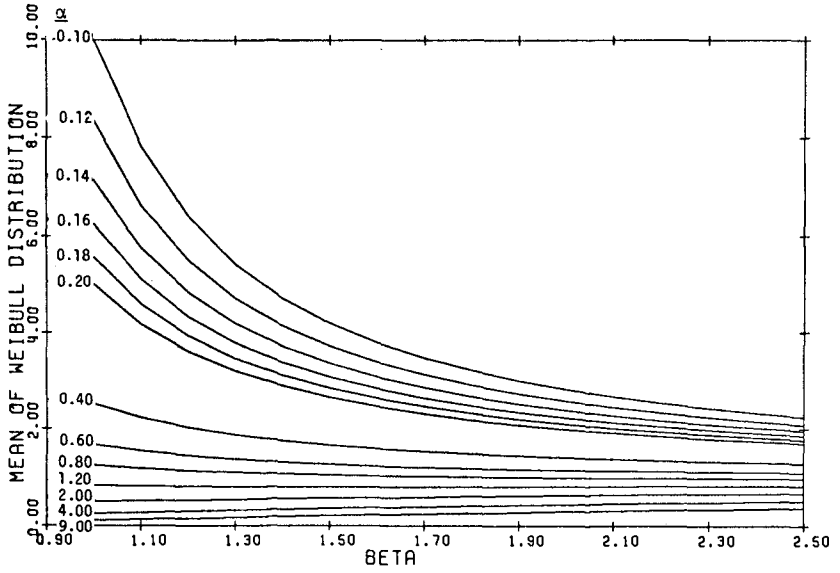

Fig. 9 Theoretical mean of Weibull distribution against β, beta for various α. (Alpha can be determined if given beta and the mean wave height.)

include the gamma function is

$$\alpha = \frac{\beta-1}{\beta} H_p^{-\beta}, \text{ or } [\alpha = \frac{\beta+1}{\beta} f_p^{\beta} \text{ where } f_p = (\frac{\beta-1}{\beta+1})^{1/\beta} T_p^{-1}] \tag{9}$$

The exact solution for the average of the largest n^{th} of waves was determined to be

$$H_{z,n/N} = \frac{N}{n} \bar{H}_z (1 - \int_0^{\ln(N/n)} f_G(y)dy) \tag{10}$$

where $y=\alpha H^{\beta}$, $\bar{H}_z$ is given by Eq. (8) and $f_G(y)$ is the incomplete gamma function ratio,

$$f_G(y) = \frac{1}{\Gamma(1+1/\beta)} e^{-y} y^{1/\beta} \tag{11}$$

An approximate solution was also obtained as

$$H_{z,n/N} = \frac{C_1}{2}[(\ln(N)/\alpha)^{1/\beta} + (\ln(N/n)/\alpha)^{1/\beta}] + C_2 \tag{12}$$

where C_1 and C_2 are arbitrary constants, and for $C_2=0$.

Then

$$\begin{aligned} H_z &= \frac{0.65}{2}[\ln(N)/\alpha]^{1/\beta} \\ H_{z,1/3} &= \frac{0.79}{2}[\ln(N)/\alpha]^{1/\beta} + (\ln(3)/\alpha)^{1/\beta}] \\ H_{z,1/10} &= \frac{0.87}{2}[\ln(N)/\alpha]^{1/\beta} + (\ln(10/\alpha)^{1/\beta}] \end{aligned} \tag{13}$$

$$H_{z,max} = 1.01[\ln(N)/\alpha]^{1/\beta} \quad (13)\ (\text{cont})$$

WAVE PERIODS

The significant period normalized by the offshore deep-water period decreases generally as waves cross the reef toward the shoreline due to the formation of multiple crests and a diminishing height to period correlation; the mean values of the ratio are:

$$\frac{T_{H_{z,1/3}}}{[T_{H_{z,1/3}}]_0} = \begin{cases} 0.704 \pm 0.176 & \text{shallow reef for offshore wind} \\ 0.642 \pm 0.168 & \text{shallow reef for onshore wind} \\ 0.853 \pm 0.110 & \text{breaker zone} \\ 0.763 \pm 0.103 & \text{outer edge of the reef (4'-8' depth)} \\ 1.000 & \text{offshore in deep water (35 ft depth)} \end{cases} \quad (14)$$

It was found that the rate of change of significant period is small and the correlation is poor (ρ_{12}=0.31).

The ratio of the average of the top third of the periods over the significant period is:

$$\frac{T_{z,1/3}}{T_{H_{z,1/3}}} = \begin{cases} 1.35 \pm 0.14 & \text{shallow reef} \\ 1.11 \pm 0.04 & \text{offshore} \end{cases} \quad (15)$$

The ratio of significant period to mean period is

$$\frac{T_{H_{z,1/3}}}{\bar{T}_z} = \begin{cases} 1.30 \pm 0.13 & \text{shallow reef} \\ 1.56 \pm 0.12 & \text{offshore} \end{cases} \quad (16)$$

The period distribution was compared to the Weibull probability denstiy function,

$$f(T) = \alpha\beta T^{\beta-1}\exp(-\alpha T^{\beta}) \quad (17)$$

which offers the best fit with correlation coefficient exceeding 0.98 in most cases. The Weibull coefficients β,α can also be found from Figs. 8 and 9 or from Eq. (5) as the periods and heights were fitted to the same distribution.

The approximate solution for the average of the largest one third of the periods is

$$T_{z,1/3} = \frac{0.77}{2}[(\ln(N/\alpha))^{1/\beta}+(\ln(3)/\alpha)^{1/\beta}] \quad (18)$$

Further, the wave periods were fitted to a symmetrical distribution presented by Longuet-Higgins (1975). The fit is poor due mainly to a positive skewness in the actual period distribution. This symmetrical distribution is generally useful for the narrow spectrum case.

WAVE SPECTRUM

The energy spectra of surf waves on the coral reef were examined in detail by: (1) Fourier spectrum analysis, and (2) zero up-crossing analysis procedures. The transformation of the Fourier spectrum as the waves cross the reef can be seen typically on Fig. 10. Offshore (probe 9), the spectrum has low energy in the high and low frequency ranges which

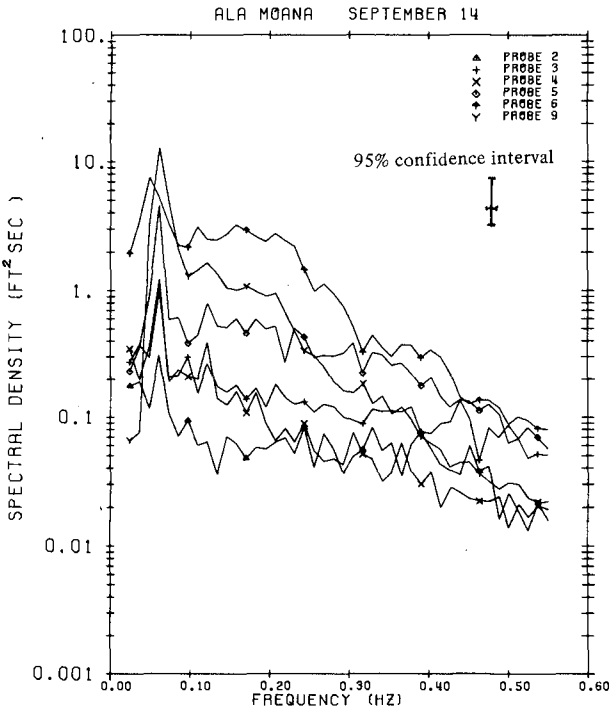

Fig. 10 Fourier spectrum for time series of 4096 data points digitized at 2.5 points per second. Each spectral estimate has 40 degrees of freedom, Ala Moana, September 14, 1976.

increases as the waves enter shallow water when energy shifts from the peak. The shift results in the production of multiple crests and periodic sea level changes at beat frequencies. Harmonics of the peak frequency are evident.

Cumulative energy (Fig. 11) and response function (Fig. 12) against position on the reef were compared. The contours of cumulative energy showing seven frequency ranges between 0 and 1.25 (Nyquist frequency) were presented so that the energy attenuation or amplification in the low, middle, and high frequency ranges can be examined in greater detail (Black, 1978). It showed that low frequency energy (below 0.05 H_z) increases from the offshore probe but it is not attenuated on the reef. Most of the energy is at frequencies less than 0.4 H_z and virtually no energy lies above 0.81 H_z. There is a decrease in variance from the offshore probe to the most seaward shallow water probe even though an increase is expected due to shoaling friction attenuates the waves over this section. The peak of the spectrum is at approximately 0.075 H_z. The peak always attenuates but high frequency energy ($0.21<f<1.25$ H_z) gains occur when waves first enter shallow water and break. The breaker zone is at approximately 380 ft from the datum (Fig. 11) where the gradient of the curves is greatest, which means there is maximum energy loss per unit distance traveled across the reef in this region. Shorewards of the breaker zone, there is attenuation at all frequencies. However, interesting behavior was noted for some days that the total variance is greater just shorewards of the breaker zone than in the breakers due to a significant increase in high frequency energy. This is caused in part by local wind-waves but it is most likely caused by wave refraction which introduces energy from the sides of the transect in this region. This suspicion is based on the fact that this phenomena was not observed in the simulated laboratory experiments (Lee, 1978).

It is interesting to note that energy gains at low frequency are larger if the offshore spectrum has a split peak due to wave-induced set-up at beat frequencies in shallow water.

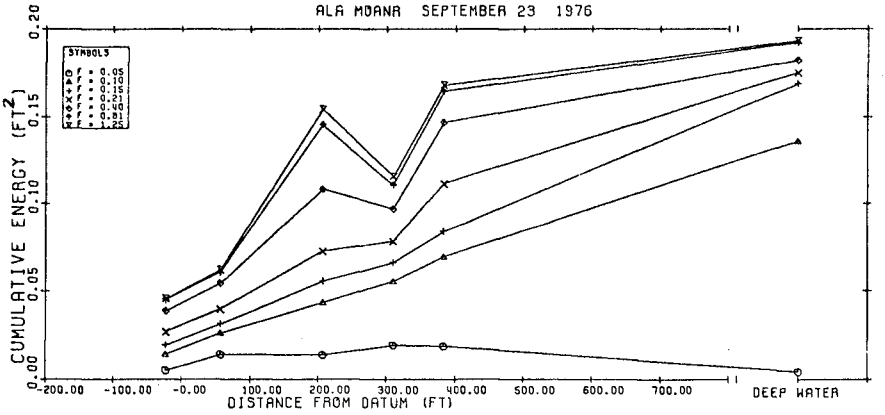

Fig. 11 Contours of cumulative energy from frequency 0.0 to F, where F is given on the symbol table, against position on the reef, Ala Moana, September 23, 1976.

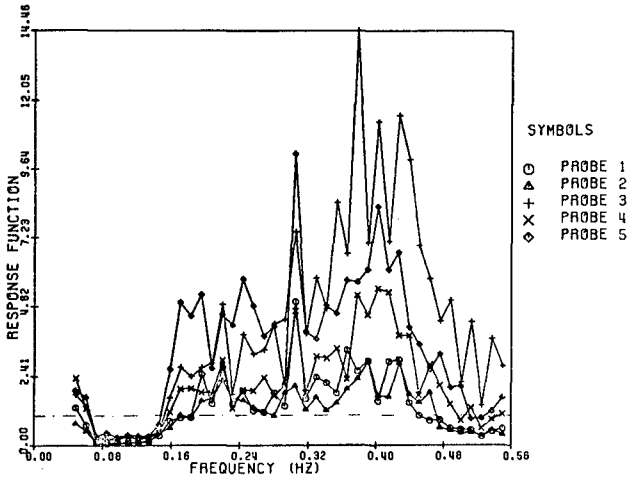

Fig. 12 Response function, R(f), against frequency, where $R(f)=S(f)_x/S(f)_9$. $S(f)_x$ is the spectral density at probe x and $S(f)_9$ is the spectral density at the offshore probe, Ala Moana, September 23, 1976.

(A) Fourier Spectrum

The period spectrum at either offshore or shallow-reef areas has the shape of Weibull distribution given by

$$S(T) = E\alpha\beta T^{\beta-1}\exp(-\alpha T^{\beta}) \tag{19}$$

where E is the total energy in the spectrum, T is the wave period, and S(T) is the spectral density (ft^2/Hz), and β,α determine the shape of the distribution and govern the spectrum peakedness.

The frequency spectrum with the shape of Weibull distribution can be obtained by a change of variable,

$$S(f) = S(T)\left|\frac{dT}{df}\right| \tag{20}$$

and

$$T = f^{-1},\ \frac{dT}{df} = -f^{-2} \tag{21}$$

then

$$S(f) = E\alpha\beta f^{-\beta-1}\exp(-\alpha f^{-\beta}) \tag{22}$$

At $f=f_p$, peak frequency

$$\frac{dS(f)}{df} = 0$$

$$f_p^{\beta} = \frac{\alpha\beta}{\beta+1} \quad \text{or} \quad \alpha = \frac{\beta+1}{\beta} f_p^{\beta} \tag{23}$$

then

$$S(f) = E\ (\frac{\beta+1}{f_p})(\frac{f}{f_p})^{-\beta-1}\exp[-(\frac{\beta+1}{\beta})(\frac{f}{f_p})^{-\beta}] \tag{24}$$

$$S(f_p) = E\ (\frac{\beta+1}{f_p})\exp[-(\frac{\beta+1}{\beta})] \tag{25}$$

To show the effect of β on the shape of the spectrum, the above equation (24) was plotted with fixed mode ($f_p=0.1$), unit variance and for $\beta=1$, 5 on Fig. 13. Note that the spectrum widens as β decreases.

Methods to obtain β will follow.

(1) Curve fitting.

The cumulative energy is

$$E_c = \int_0^f S(f)df = E\exp(-\alpha f^{-\beta}) \tag{26}$$

and taking logarithms twice gives

$$\ln[\ln(E/E_c)] = \ln(\alpha) - \beta\ln(f) \tag{27}$$

which is a linear equation with intercept at $\ln(\alpha)$ and gradient $-\beta$.

(2) Iteration.

A simple method was developed to determine β, without curve-fitting, from Eq. (25) using a simple iterative technique.

$$\exp[(\frac{\beta+1}{\beta})]/(\beta+1) = E/[S(f_p)\cdot f_p] \tag{28}$$

With the peak frequency (f_p), energy density at peak frequency [$S(f_p)$], and the total energy in the spectrum E, β can be obtained. This relationship was plotted on Fig. 14, and β may be obtained by

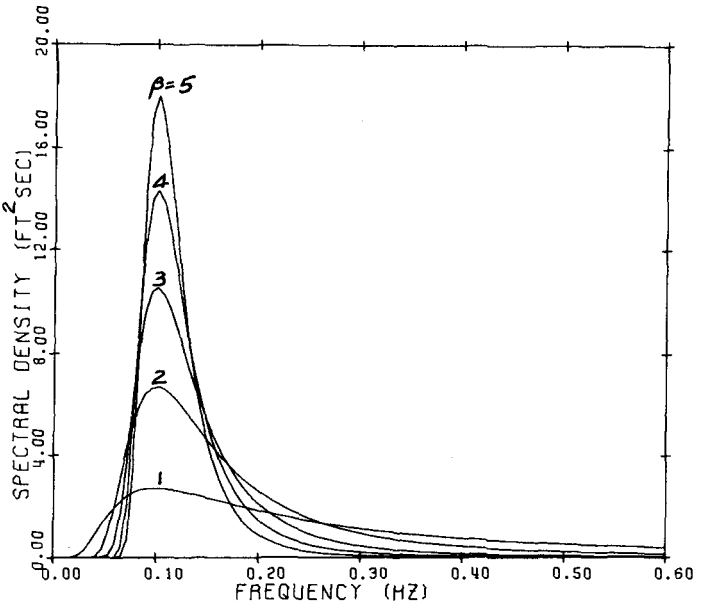

Fig. 13 Theoretical spectra with the shape of Weibull distribution with unit variance, peak frequency f_p=0.1 H_z and for β=1,5.

entering the function $E/[S(f_p)\cdot f_p]$. The other coefficient, α, may be obtained by

$$\alpha = \frac{\beta+1}{\beta} f_p^{\beta} \qquad (29)$$

Analysis showed that the spectrum found in this manner fits the peak exactly but does not necessarily describe the rest of the spectrum well. This method should only be used when an "easy-to-obtain" estimate of β is required or if the spectrum has been highly smoothed. In general, the value of β by iteration is greater than that by curve-fitting.

(3) Goda's spectral peakedness parameter.

Another alternative method to obtain β without curve-fitting employs Goda's spectral peakedness parameters Q_p (Goda, 1974).

$$Q_p = \frac{2}{m_0^2} \int_0^{\infty} f\, S(f)^2 df \qquad (30)$$

where m_0 is zeroth spectral moment.

It can be shown for a spectrum with the shape of the Weibull distribution that (Black, 1978)

$$Q_p = \beta/2 \qquad (31)$$

In which case, the peakedness β can be found using Q_p.

It was found that Q_p represents the shape of the spectrum much better than the spectral width parameter

$$\varepsilon_s = \sqrt{1 - \frac{m_2^2}{m_0 m_4}} \quad \text{or} \quad \varepsilon_T = \sqrt{1 - \left(\frac{N_z}{N_c}\right)^2}$$

The spectral width parameters vary considerably with the high frequency cut-off choice, therefore, they are not a good parameter to characterize the spectral distribution.

The design frequency spectrum for engineering applications on coral reef environment is recommended as follows:

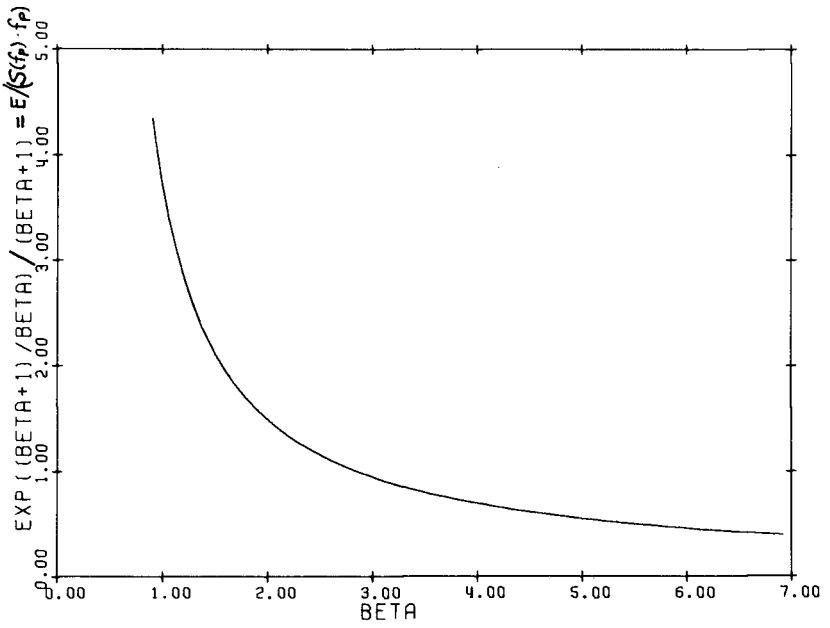

Fig. 14 Theoretical curve to obtain Beta for the spectrum with the shape of the Weibull distribution using the peak energy density, where $\exp(\beta+1/\beta)/(\beta+1)=E/(S(f_p)\cdot f_p)$ and E is total energy in spectrum, f_p is peak frequency and $S(f_p)$ is energy density at peak.

(a) Swell spectrum (offshore 35 ft depth)

$$S(f) = 4E_1 f_p^{-1}(f/f_p)^{-4}\exp[-\tfrac{4}{3}(f/f_p)^{-3}] \tag{32}$$

(b) Shallow water on the offshore side of the reef (5 ft depth)

$$S(f) = 3E_2 f_p^{-1}(f/f_p)^{-3}\exp[-\tfrac{3}{2}(f/f_p)^{-2}] \tag{33}$$

(c) Shallow water on the shoreward side of the reef (3 ft depth)

$$S(f) = 2E_3 f_p^{-1}(f/f_p)^{-2}\exp[-2(f/f_p)^{-1}] \tag{34}$$

In all three cases f_p is the offshore peak frequency and the total energy $E=(1/4\ H_{z,1/3})^2$ where $H_{z,1/3}$ is significant wave height.

The normalized non-dimensional frequency spectrum has the general form of

$$\frac{S(f)}{S(f_p)} = [\exp(\tfrac{\beta+1}{\beta})](f/f_p)^{-\beta-1}\exp[-(\tfrac{\beta+1}{\beta})(f/f_p)^{-\beta}] \tag{35}$$

Then, the normalized design frequency spectra are:

(a) Normalized swell frequency spectrum (offshore 35 ft depth)

$$\frac{S(f)}{S(f_p)} = [\exp(\tfrac{4}{3})](f/f_p)^{-4}\exp[-\tfrac{4}{3}(f/f_p)^{-3}];\ \beta=3 \tag{36}$$

(b) Normalized design frequency spectrum for shallow water on the offshore side of the reef (5 ft depth)

$$\frac{S(f)}{S(f_p)} = [\exp(\tfrac{3}{2})](f/f_p)^{-3}\exp[-\tfrac{3}{2}(f/f_p)^{-2}];\ \beta=2 \tag{37}$$

(c) Normalized design frequency spectrum for shallow water on the shoreward side of the reef (3 ft depth)

$$\frac{S(f)}{S(f_p)} = [\exp(2)](f/f_p)^{-2}\exp[-2(f/f_p)^{-1}];\ \beta=1 \tag{38}$$

These non-dimensional design frequency spectra are plotted on Fig. 15 and they are compared with the following well-known Bretschneider frequency spectrum with $\beta=4$ for deep water,

$$\frac{S(f)}{S(f_p)} = [\exp(\tfrac{5}{4})](f/f_p)^{-5}\exp[-\tfrac{5}{4}(f/f_p)^{-4}] \tag{39}$$

The normalized non-dimensional period spectrum can be obtained from Eq. (19),

$$S(T) = E\alpha\beta T^{\beta-1}\exp(-\alpha T^{\beta})$$

At $T = T_p$

$$\frac{dS(T)}{dT} = 0 \qquad T_p^{-\beta} = \frac{\alpha\beta}{\beta-1} \qquad \text{then} \quad \alpha = \frac{\beta-1}{\beta}T_p^{-\beta}$$

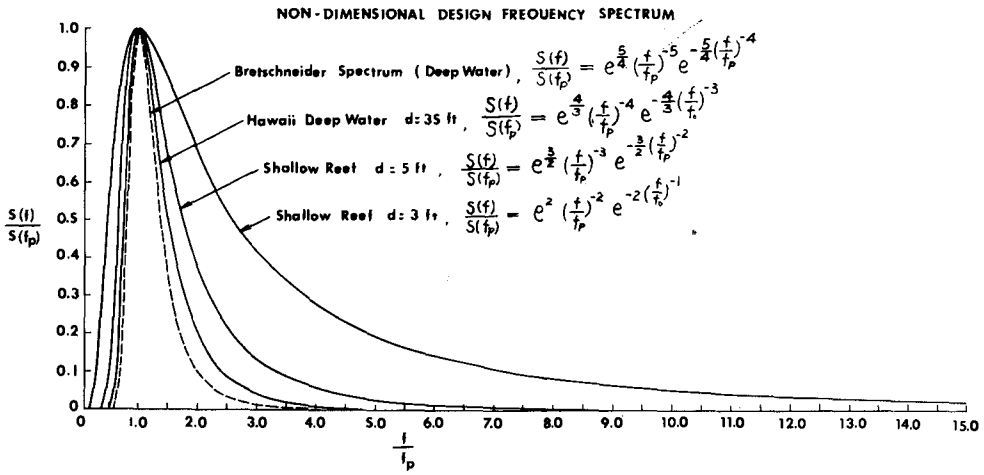

Fig. 15 Non-dimensional design frequency spectra

Then

$$S(T) = E(\beta-1)T_p^{-1}(T/T_p)^{\beta-1}\exp[-(\frac{\beta-1}{\beta})(T/T_p)^{\beta}] \quad (40)$$

$$S(T_p) = E(\beta-1)T_p^{-1}\exp[-(\frac{\beta-1}{\beta})] \quad (41)$$

The non-dimensional period spectrum has the general form of

$$\frac{S(T)}{S(T_p)} = [\exp(\frac{\beta-1}{\beta})](T/T_p)^{\beta-1}\exp[-(\frac{\beta-1}{\beta})(T/T_p)^{\beta}] \quad (42)$$

Then, the normalized design period spectra are:

(a) Normalized swell period spectrum (offshore 35 ft depth)

$$\frac{S(T)}{S(T_p)} = [\exp(\frac{2}{3})](T/T_p)^2\exp[-\frac{2}{3}(T/T_p)^3] \quad (43)$$

(b) Normalized design period spectrum for shallow water on the offshore side of the reef (5 ft depth)

$$\frac{S(T)}{S(T_p)} = [\exp(\frac{1}{2})](T/T_p)\exp[-\frac{1}{2}(T/T_p)^2] \quad (44)$$

The Bretschneider normalized period spectrum is

$$\frac{S(T)}{S(T_p)} = [\exp(\frac{3}{4})](T/T_p)^3\exp[-\frac{3}{4}(T/T_p)^4] \quad (45)$$

The shape of the period spectrum was compared in Fig. 16.

Note that the peak frequency is related to the peak period as follows:

$$f_p^{-1} = (\frac{\beta+1}{\beta-1})^{1/\beta}\, T_p \quad (46)$$

The relationship between the spectrum and zero up-crossing period statistics was established and compared with others as listed in Table 1.

Ratio	Subject Study			Goda [1974]	Haring et al. [1976]	Manohar et al. [1976]
	range	shallow	offshore			
$\overline{T}_z/T_p$	0.22-0.58	0.38±0.09	0.46±0.08	0.75	0.52	
$T_{Hz,1/3}/T_p$	0.28-0.80	0.49±0.13	0.71±0.12	0.94	0.75	0.78
$T_{Hz,1/10}/T_p$	0.29-0.91	0.54±0.15	0.80±0.10		0.76	
$T_{Hz,max}/T_p$	0.23-1.03	0.66±0.31	0.89±0.11		0.77	
$T_{Hz,1/3}/T_{m01}$	1.02-2.24	1.47±0.30	1.29±0.06	1.30	1.33	
$\overline{T}_z/T_{m02}$	1.13-2.46	1.62±0.30	1.16±0.03	1.20	1.15	

Table 1 Range, shallow water and offshore mean values with standard deviations, and comparison with other workers, of Ala Moana results, 1976.

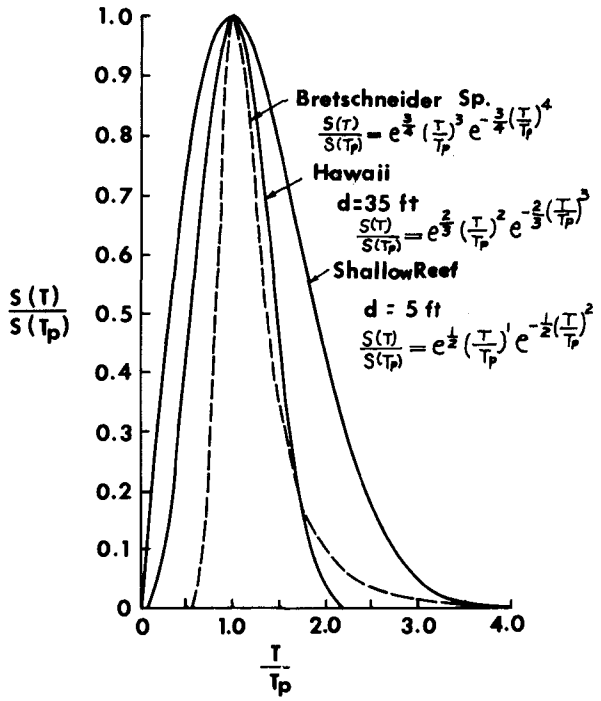

Fig. 16 Non-dimensional design period spectra

Note that the ratios are significantly reduced by shallow water. This occurs because the peak period of the spectrum is usually constant but the zero up-crossing periods are reduced due to the shifting of energy into the high frequency range. The standard deviation or scattering in the data is much greater in shallow water than offshore.

The spectrum contains a height to period relationship which is linearly dependent on the first spectrum moment (m_1). The best-fit equation with excellent correlation coefficient $P_{12}=0.975$, is

$$\overline{H}_z^2/\overline{T}_z = 4.828\, m_1 \qquad (47)$$

Furthermore, comparison of the spectrum peakedness and the peakedness of the period distribution produced linear correlation. A peaked spectrum (large β) should correspond to a peaked period distribution.

(B) Zero up-crossing spectrum (ZUS)

The zero up-crossing spectrum (ZUS) is defined as

$$S(f) = g(f)\cdot\frac{1}{8}H^2_{rms}(f) \qquad (48)$$

which states that the energy density at frequency f is equal to one eighth the square of the zero up-crossing root mean square wave height at that frequency multiplied by the probability that frequency f will occur in the record. For the discrete case

$$S(f) = \frac{\sum_{i=1}^{m} H_i^2(f)}{8N\cdot\Delta f} \qquad (49)$$

where Δf is the frequency interval and includes waves with frequencies from $f-\Delta f/2$ to $f+\Delta f/2$; N is the total number of waves in the record; m is the number of waves of zero up-crossing height H_i with frequencies that lie in the interval defined above. The definition states that the energy is large in a band if many waves fall in the band and if the amplitude of those waves is large.

Under the above definition, the energy of each wave is assumed to be $H^2/8$ which is only true for sinusoidal waves. It is not essential to do

this as $H_i^2(f)/8$ can be replaced by $E_i(f)$ where E_i is the variance of the time series between the two zero up-crossings which defined the height $H_i(f)$. For simplicity, the definition of $H^2/8=E$ is retained here.

The confidence interval for each estimate is

$$\log S(f) + \log m/\chi_m(\alpha/2) \ , \quad \log S(f) + \log m/\chi_m(1 - \alpha/2) \tag{50}$$

at the $1 - \alpha/2$ confidence level, where χ_m is Chi-squared with m degrees of freedom.

The Fourier spectrum (FS) and ZUS are compared on Fig. 17. It showed that the FS and ZUS have distinct similarities but cannot be considered identical. The ZUS is more peaked than the FS. The ZUS allocates most energy over a narrower range than the FS, due to the fact that the zero up-crossing technique selects waves in this range. The ZUS is less stable away from the peak where the number of occurrences in each band decreases and the confidence widens.

The major advantage of the ZUS is that linearity is not required. Because each zero up-crossing wave is isolated from its neighbors, when the spectrum is considered in this manner the problem of interpretation of sinusoidal components at harmonic frequencies in a non-linear environment does not arise. This is useful for shallow water applications. Another advantage is that the spectrum contains a height to frequency relationship which is easily retrieved from the spectrum as

$$H_{rms}^2(f) = \frac{8N \cdot \Delta f \cdot S(f)}{m} \tag{51}$$

The major disadvantage is that if one only had the ZUS it would not be possible to recreate the time series, as the spectrum contains no information about the order in which waves occur. This is unfortunate for

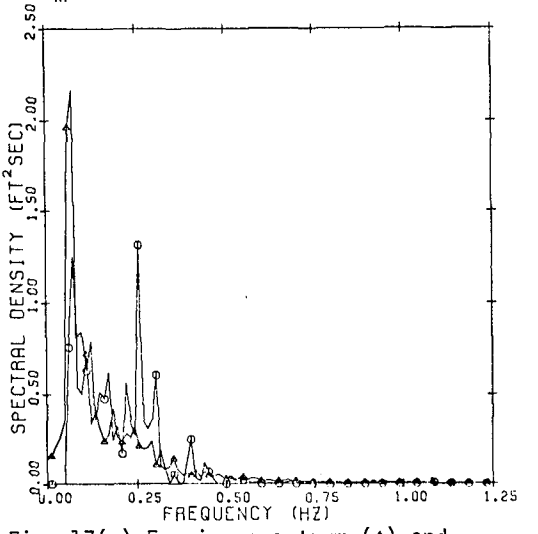

Fig. 17(a) Fourier spectrum (Δ) and ZUS (o) for September 7, probe 5, Ala Moana, 1976.

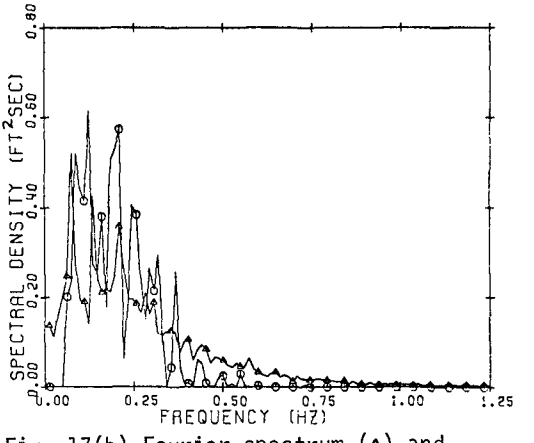

Fig. 17(b) Fourier spectrum (Δ) and ZUS (o) for September 7, probe 3, Ala Moana, 1976.

applications where a spectrum is used to generate a sea surface for theoretical studies. Other disadvantages are critisims aimed at the zero up-crossing procedure in general.

The ZUS is a useful tool for describing ocean waves. For engineering applications, the zero up-crossing analysis in general has some specific advantages and the ZUS is an extension of this approach. It shows the energy partition in a fashion similar to the Fourier spectrum and one can obtain all the statistics such as the significant wave height and period, etc. during the analysis. These cannot be easily obtained in shallow water from the Fourier spectrum.

The ZUS was fitted to the shape of the Weibull distribution given by

$$S(f) = E\alpha\beta f^{-\beta-1}\exp(-\alpha f^{-\beta}) \tag{52}$$

The peakedness, β, varies from 2.17 to 4.18 and is largest just seaward of the breaker zone.

The best-fit ZUS spectrum with Weibull distribution can be used to obtain period parameters from the following relationships

$$T_{m01} = m_0/m_1 = \frac{\alpha^{-1/\beta}}{\Gamma(1 - 1/\beta)} \tag{53}$$

$$T_{m02} = (m_0/m_1)^{1/2} = \frac{\alpha^{-1/\beta}}{\Gamma(1 - 2/\beta)} \tag{54}$$

The relationship of mean period ($\bar{T}_z$) from the zero up-crossing analysis to mean period (T_{m01}) of the ZUS, and to mean apparent period (T_{m02}) of the ZUS are given as follows:

$$\bar{T}_z/T_{m01(ZUS)} = \begin{array}{ll} 1.106 \pm 0.122 & \text{shallow reef} \\ 0.826 \pm 0.061 & \text{offshore} \end{array} \tag{55}$$

$$\bar{T}_z/T_{m02(ZUS)} = \begin{array}{ll} 1.303 \pm 0.189 & \text{shallow reef} \\ 0.977 \pm 0.085 & \text{offshore} \end{array}$$

It was shown that the peak of the ZUS occurs at or near the peak of the wave frequency distribution so that the confidence is best near the ZUS peak.

In summary, both the ZUS and Fourier spectra are used to test the adequacy of formulae which estimate individual wave parameters. The results for shallow water deviate significantly from the Rice's (1944 and 1945) theory, which is often used to estimate period statistics.

(C) Cross Spectrum

Cross spectra analysis was made to obtain gain function and required coherency for all time series between the adjacent shallow water probes on the reef. It was found that the squared coherency is close to unity near the peak frequency. This means that the output spectrum near the peak can be predicted from the input by applying the gain function because the system is linear in this frequency range. However, the squared coherency was extremely small for other frequencies above 0.25 H_z. There are energy gains from the probe in the breakers to the next probe shorewards in the mid-frequency range. The relative phase of the two adjacent time series showed that the waves were non-dispersive below approximately 0.25 H_z in shallow water. Typical squared coherency and gain function as a function of probe position on the reef is shown in Fig. 18.

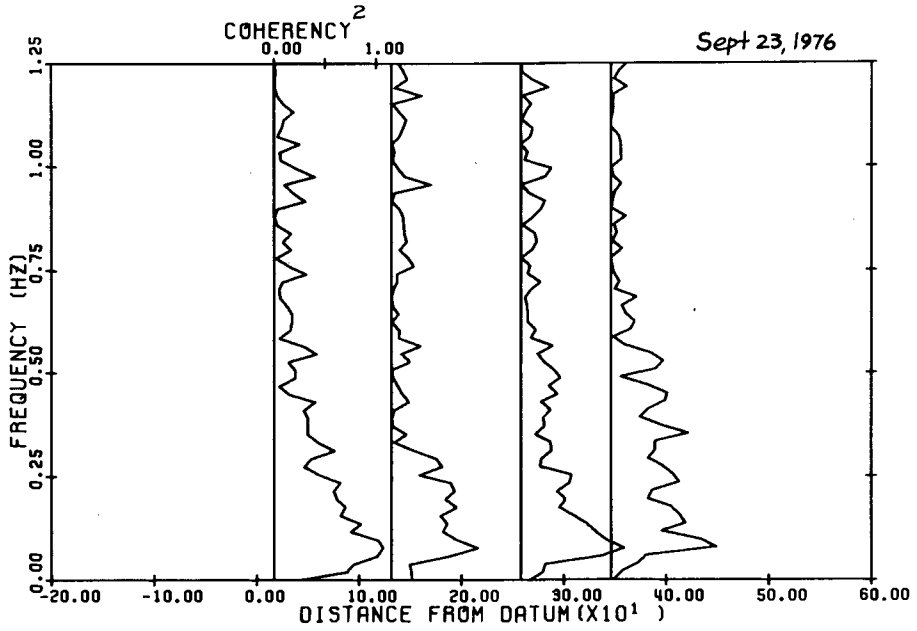

Fig. 18(a) Squared coherency, Ala Moana, September 23, 1976.

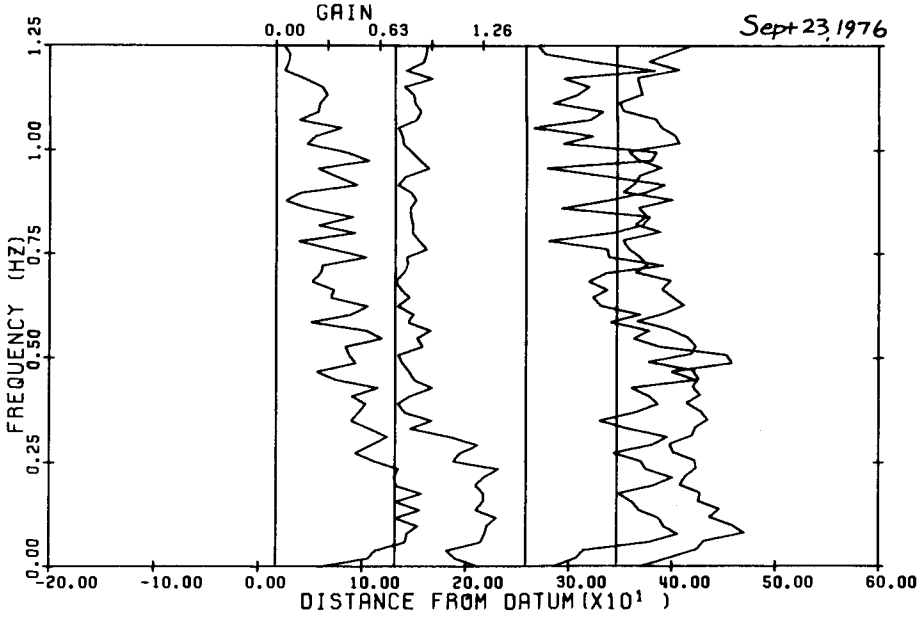

Fig. 18(b) Gain function, G(f), Ala Moana, September 23, 1976.

REFERENCES

Arham, M., and R. Ezraty (1975), "Saisie et Analyse de Données des Courants Particulaires au Voisinage du Fond Dans La Houle Littorale Proche du Deferlement," La Houille Blanche No. 7/8, 1975, p. 484-496.

Black, K.P. (1978), "Wave Transmission Over Shallow Reef (Field Measurements and Data Analysis," Tech. Rep. 78-42, J.K.K. Look Laboratory of Oceanographic Eng., Univ. of Hawaii, March 1978 (Also published as M.S. thesis, "Wave Transformation on a Coral Reef," Univ. of Melbourne, Aust., April 1978).

Battjes, J.A. (1972), "Set-up Due to Irregular Waves," Proc. of 13th International Conference on Coastal Eng. (July 10-14, 1972, Vancouver, Canada), ASCE, N.Y., 1972, p. 1993-2004.

Bushing, F. (1976), "Energy Spectra of Irregular Surf Waves," Proc. of 15th International Conference on Coastal Eng. (July 1976, Honolulu), ASCE, p. 539-559.

Goda, Y. (1974), "Estimation of Wave Statistics from Spectral Info.," Proc. of Int. Symp. on Ocean Wave Measurement and Analysis," (Sept. 1974, New Orleans), ASCE.

Haring, R.E., A.R. Osborne and L.P. Spenser (1976), "Extreme Wave Parameters Based on Continental Shelf Storm Wave Record," Proc. of 15th Int. Conf. on Coastal Eng. (July 1976, Honolulu), ASCE, p. 151-170.

Kuo, C.T. and S.T. Kuo (1975), "Effect of Wave Breaking on Statistical Distribution of Wave Heights," Proc. of Civil Eng. in the Oceans III, Vol. 2, p. 1211-1231.

Lee, T.T. (1978), "Wave Transmission over Shallow Reef (Laboratory Simulation)," Tech. Report 78-44, J.K.K. Look Laboratory of Ocean. Eng., December 1978 (in preparation).

Longuet-Higgins, M.S. (1975), "On the Joint Distribution of the Periods and Amplitudes of Sea Waves," Jour. Geophys. Res., Vol. 80, No. 18, p. 2688-2694.

Manohar, M., I.E. Mobarek and N.A. El. Sharaky (1976), "Characteristic Wave Period," Proc. of 15th Int. Conf. on Coastal Eng. (July 1976, Honolulu), ASCE, Vol. 1, p. 273-288.

Rice, S.O. (1944 and 1945), "Mathematical Analysis of a Random Noise," Bell Systems Tech. Jour., Vol. 23, p. 184-294, 1944; and Vol. 24, p. 133-183, 1945.

ACKNOWLEDGMENTS

This study was jointly supported by Sea Grant, NOAA, the Governor's Office of Marine Affairs, University of Melbourne, and the University of Hawaii. Dr. Edward Thornton of the U.S. Naval Postgraduate School and Dr. J.A. Battjes of the University of Technology, Delft, provided technical assistance while they were at the University of Hawaii as Visiting Colleagues during the academic year 1975-1976 and summer 1976, respectively. Professor F. Gerritsen and George Weber assisted greatly during the course of study.